

Article

# Development of Body Tissue Temperature Control Transducer

Audrone Dumciene <sup>1</sup> and Saule Sipaviciene <sup>2</sup>

<sup>1</sup>Department of Health, Physical and Social Education, Lithuanian Sports University,  
Sporto St. 6, LT-44221 Kaunas, Lithuania; audrone.dumciene@lsu.lt

<sup>2</sup>Department of Applied Biology and Rehabilitation, Lithuanian Sports University,  
Sporto St. 6, LT-44221 Kaunas, Lithuania; saule.sipaviciene@lsu.lt

\* Correspondence: audrone.dumciene@lsu.lt; Tel.: +370-698-277-66

**Abstract:** The aim of the study was to evaluate the influence of transducer design and its elements, and their materials on temperature in deeper layers of tissues measurement results. A digital modeling was performed to evaluate the influence of the properties of transducer design elements. Experimental research was carried out. Revealed that the accuracy, similar to that of an invasive method using needle probes, can be achieved by measuring the temperature in deeper muscle layers using the proposed transducer.

**Keywords:** body temperature; sensors; transducer

---

## 1. Introduction

Several concepts are used in human body temperature measurements: core body temperature, body temperature, muscle temperature, body skin temperature et. all.

The functioning of the body temperature measuring devices is based on various physics principles (non-electric, thermoelectric, resistance, impedance, semiconductors, fibre optic, ultrasonics et all.) but as gear, they can be divided into two groups: non-invasive, whether natural body openings are used for temperature measurement, and invasive, whether an invasion in human body is necessary. The most accurate core body temperature can be measured by gear known as the Schwan-Ganz catheter, which is invasively introduced into the pulmonary artery or measured in by esophageal catheter inserted in oesophagus [1]. The core body temperature of healthy people is range of  $37\text{ }^{\circ}\text{C} \pm 0.6\text{ }^{\circ}\text{C}$  which can be changed with circadines rhythms. This temperature is assumed to be a relatively standard and is called the "gold standard".

For precise non-invasive body temperature measurement most commonly are used tympanic ear and rectal thermometers [2, 3, 4]. Same studies have shown that normal body temperature ranges can be between  $36.2$  and  $37.5\text{ }^{\circ}\text{C}$  [5].

Non-invasive measurements of human body temperature utilize various digital medical thermometers, in which temperature sensors are commonly used in thermistors. Known and referred to as "zero heat flow" (ZHF) temperature gauges with a heat source to create a heat flow equilibrium [6] and gauges with two sensors that do not require a heat source [7]. They are used in various studies [8]. The MRI method [9] and the multi-frequency impedance method [10] are used to monitor the distribution of temperature fields in the tissues.

The most common tools used for measuring skin temperature are contactless infrared and conductive devices [11, 12]. For measuring the temperature in deeper layers of tissues, needle thermometers are usually used, which are inserted into tissues 3-4 cm in length [13, 14]. The needle thermometers must be sterilized before use and disinfected after use. The measurement procedure is not "pleasant" to the subject.

## 2. Materials and Methods

In [15] was shown, that muscle temperature can be measured using multi-sensory transducer. This time, we discuss new design of multi-sensory transducer, which structures are shown on Figure 1, because the thermal channel and isolation cover dimension, and the influence of channel material have not been clarified.

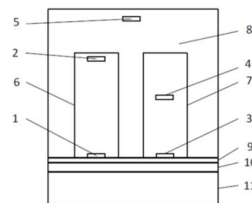


**Figure 1.** Transducer structures. (a) there 1, 2, 3, 4, 5 – temperature sensors (thermistor 5 can be used to inspect the thermo-isolation cover); 6 – thermal channel; 7 – thermal channel; 8 – thermo-insulation cover; 9 – skin; 10 – fat; 11 – muscle.

The thermal equivalent circuit of the Transducer shown in Figure 1, without considering the influence of the thermistors, can be formed as shown in Figure 2.

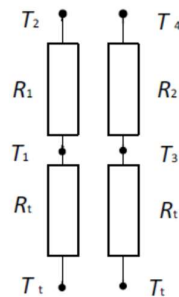


**Figure 2.** Equivalent resistances circuit of two heat flow channels

There  $T_t$  – tissue deep layer's temperature,  $T_1$  – sensor's 1 temperature,  $T_2$  – sensor's 2 temperature,  $T_3$  – sensor's 3 temperature, and  $T_4$  – sensor's 4 temperature,  $R_t$  – tissue thermal resistance,  $R_1$  – thermal resistance of one thermal channel,  $R_2$  – thermal resistance of other thermal channel

The human body, using nutrients, generates bioheat. Due to the flow of blood and due to the heat transfer process, the heat is transferred into entire body until it is balanced with the environment. The description of the heat propagation in living organisms is most often used by the Pennes [16] equation or its modifications, which assess the specific conditions [17]. Using the Pennes' equation and the boundary conditions established for the variant under consideration, one can simulate the heat propagation process in the human body and calculate the distribution of temperature fields.

So, the bioheat transfer process in human body can be described by equation [16]

$$\delta_{ts} \rho C \frac{\delta T}{\delta t} + \nabla \cdot (-k \nabla T) = \rho_b C_b \omega_b (T_b - T) + Q_m + Q_{ex} \quad (1)$$

where:  $\delta_{ts}$  – a time-scaling coefficient (dimensionless);  $\rho$  – the tissue density ( $\text{kg/m}^3$ );  $C$  – the specific heat of tissue ( $\text{J}/(\text{kg}\cdot\text{K})$ );  $k$  – the tissue's thermal conductivity tensor ( $\text{W}/(\text{m}\cdot\text{K})$ );  $\rho_b$  – the density of blood ( $\text{kg/m}^3$ );  $C_b$  – the specific heat temperature (K);  $Q_{met}$  – the heat source from metabolism ( $\text{W/m}^3$ );  $Q_{ex}$  – the spatial heat source in body of blood ( $\text{J}/(\text{kg}\cdot\text{K})$ );  $\omega_b$  – the blood perfusion rate ( $\text{m}^3/(\text{m}^3\cdot\text{s})$ );  $T_b$  – the arterial blood temperature (K);  $T$  – ( $\text{W/m}^3$ ).

We are investigating the case when a person is in a state of rest and at a relatively stable ambient temperature. In this case, we can write

$$\nabla \cdot (-k \nabla T) = \rho_b C_b \omega_b (T_b - T) + Q_m + Q_{ex} \quad (2)$$

If person is in a state of rest, we can accept that  $Q_{ex} = 0$  and transform equation (2) as

$$\nabla \cdot (-k \nabla T) = \rho_b C_b \omega_b (T_b - T) + Q_m \quad (3)$$

Therefore, equation (2) can be used to simulation of temperature fields in tissues. We are interested in distribution of temperature fields in tissues and in transducer body.

Since the volume of transducer is small compared with parts of the human body in which the temperature will be measured the accuracy is reduced using equation (2) for propagation of heat in the transducer body.

Boundary conditions:  $-\vec{n} \cdot (-k \nabla T) = q_0 + h(T_{ext} - T)$  – heat flux (external boundary of the tissue and transducer model);  $\vec{n} \cdot (k_1 \nabla T_1 - k_2 \nabla T_2) = 0$  – continuity on the all interior boundary between layers of the tissue and transducer body model;  $-\vec{n} \cdot (-k \nabla T) = 0$  – using the symmetry of the object under study, the symmetry condition is asked. (4)

The human tissue model properties [18] used in simulation are given in Table 1.

**Table 1.** Human tissue layer's properties

Layer	$\rho$ ( $\text{kg/m}^3$ )	$k$ ( $\text{W/m}\cdot\text{K}$ )	$C_p$ ( $\text{J/kg}\cdot\text{K}$ )	Thickness m	$Q_{met}$ ( $\text{W/m}^3$ )	$\omega_b$ (1/s)	$T_b$ (K)
Muscle	1090	0.5	3766	0.12	5	0.0001	310.15
Fat	850	0.16	2510	0.0025	0	4/5e-6	310.15
Skin	1100	0.21	3250	0.002	4	7.2e-8	310.15
Blood	1050	0.32	1313	0.03		0.5	310.15

The *COMSOL Multiphysics* 3.5. software package was used to simulate temperature fields in the tissues and transducer body at environment temperature 20 °C.

The precision Cantherm thermistors type MF51E103F3380 with time constant  $\leq 3.2$  seconds were used as temperature sensors which are intended for medical equipment. For thermistors was

conducted calibration procedure and Steinhart-Hart equation was used as equation of resistance temperature  $R(T)$  characteristics approximation. The equation can be written as follows:

$$1/T = B_0 + B_1 \ln R_T + B_3 (\ln R_T)^3 \quad (5)$$

were  $T$  – the temperature in degrees K;  $B_0$ ,  $B_1$ , and  $B_3$  are the equation's coefficients and  $R_T$  is the thermistor resistance at the temperature  $T$ .

Coefficients  $B_0$ ,  $B_1$ , and  $B_3$ , have been estimated from a thermistor calibration results, since the  $R(T)$  characteristics from the manufacturer are not for individual thermistors, but averaged thermistor type MF51. The accuracy of calibrated thermistors after applying the linearization of Steinhart-Hart equation was in range  $\pm 0.02$  °C.

The structure of physical model used for transducer examination is shown in Figure 3.

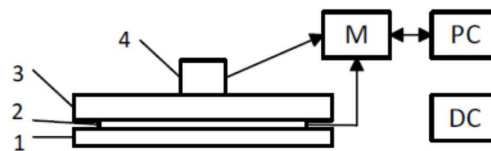


**Figure 3.** The structure diagram of experiment

Where 1 – cooler; 2 – Peltier element; 3 – polyethylene plate; 4 – transducer; M – Temperature meter; PC – laptop; DC – DC source

Temperature in six points was measured using the FLUKE thermometer type Black Stack 1560 and Thermistor readout module type 2564. Reference temperature at the top of the polyethylene plate was maintained within the range of  $30 \pm 0.1$  °C.

The temperature of transducer sensors 1, 2, 3, 4, 5 was measured using, as noted above, Fluke thermometer. The temperature on the boundary between plate surface and transducer pad can be calculated using the equation [15], modified as follows

$$T_t = \frac{T_1 (\lambda (T_3 - T_4) - T_3 (|T_1 - T_2|))}{\lambda (T_3 - T_4) - (|T_1 - T_2|)} \quad (6)$$

Were  $T_1$ ,  $T_2$ ,  $T_3$  and  $T_4$  – temperature at points shown in Figure 2;  $\lambda$  – ratio of thermal channel thermal resistance  $R_1/R_2$ .

As shown in [15], that this ratio must be more than four. So, the ratio of thermal resistors  $R_1$  and  $R_2$  of the thermal channels was chosen to be equal to five.

To calculate the tissue temperature at a depth of 3 cm can be used the equation [15]

$$T = 0.5026 * T_{ss} + 18.399, \quad (7)$$

were  $T_{ss}$  – temperature on skin surface measured by transducer.

The dimension of thermal channel and thermo-isolation cover is shown in Figure 4.

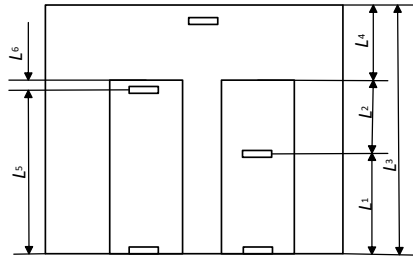


**Figure 4.** Main dimension of transducer elements

Dimensions  $L_1$ ,  $L_2$ ,  $L_3$ ,  $L_4$ ,  $L_5$  and  $L_6$ , shown in Figure 2, are used as variables by simulating the distribution of temperature fields in a transducer.

The hard plastic cover and polyurethane foam for thermos-isolation and epoxy with cooper powder were used for transducer design.

Ethical approval for experiment with human was granted by the Kaunas regional biomedical research ethics committee (Protocol No 1–60/2004) and the measurement was completed in accordance with the Helsinki Declaration.

It was one volunteer and for temperature in deep muscle measurement was used thermometer type MKA (Ellab A/S, type DM 852, Denmark) with needle probe.

### 3. Results

The distribution of temperature fields in the tissue-transducer models (Figure 1), at different variables  $L_1$ ,  $L_2$ ,  $L_3$ ,  $L_4$ ,  $L_5$ , and  $L_6$  values, when the environment temperature was  $+20\text{ }^{\circ}\text{C}$ , for illustration purposes is given in Figure 5 (a, b c for different variables values).

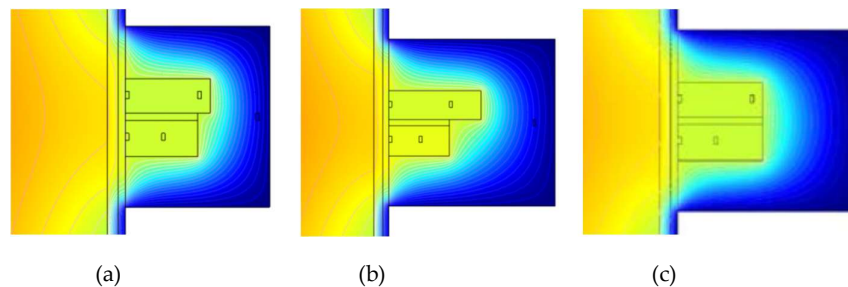


**Figure 5.** Distribution of temperature fields in tissues and transducer.

The results of simulation of influence of the thermal conductivity of materials the thermal channels' in the temperature of the material on the boundary between the tissue surface and transducer pad are shown in Figure 6.

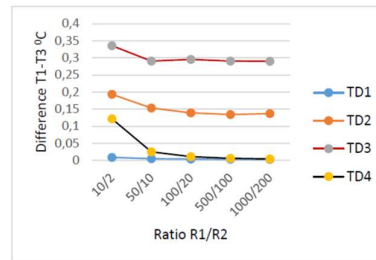


**Figure 6.** The influence of the thermal conductivity of materials the thermal channels' in the temperature of the material on the boundary between the tissue surface and transducer pad

In the evaluation of simulation results, Figure 6, it can be concluded that for the purpose of obtaining a lower transducer temperature time constant, materials for a thermal channel are required which have a thermal conductivity of from 500/100 to 1000/200 (were the thermal conductivity coefficient of the short channel material is in fraction denominator and of the longer channel in counter).

The results of optimization of the thermal insulation cover thickness  $L_3$  (Fig. 4) as function of difference temperature  $T_1$  and  $T_3$  are shown in Figure 7.

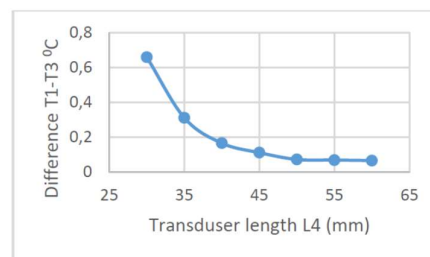


**Figure 7.** The influence of length  $L_3$  on difference T1-T2

The results of simulation of influence of the thermal insulation cover thickness  $l_6$  (Fig. 4) on temperature on boundary between the tissue surface and transducer pad are shown in Figure 8.

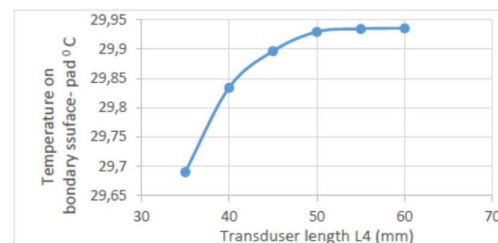


**Figure 8.** The influence of length  $L_4$  on temperature on the boundary between the tissue surface and transducer pad

The physical experiment with transducer was repeated 10 times. Measured sensors' average temperatures were  $T_1=30.367\pm 0.0091$  °C,  $T_2=30.161\pm 0.0096$  °C,  $T_3=30.199\pm 0.0087$  °C and  $T_4=29.4521\pm 0.0108$  °C. The temperature  $T_q$  on the boundary between the tissue surface and transducer

pad can be calculated using equation (6) and the values of measured temperatures for  $T_1$ ,  $T_2$ ,  $T_3$  and  $T_4$ . The estimated temperature  $T_{sp}$  of the experiment, it was  $T_{cp} = 30.199$  °C. So, it is possible to say, that calculated and reference temperatures vary within the range of  $\pm 0.2$  °C.

The temperature at the tissue depth of 3 cm, calculated using equation (7) and estimated temperature value  $T_{cp}$ , it was 33.58 °C.

The thigh's surface (skin) temperature of volunteer in lying position was measured with the transducer. The transducer was placed on thighs. Next to the transducer, at distance 10-mm from transducer sterile gauge MKA needle probe was inserted into the 30 mm deep. The room temperature during the experiment was  $20 \pm 1$  °C. After waiting for one minute both thermometer MKA and transducer measured values did not change practically and were recorded. Muscle temperature measured by thermometer type MKA it was 36.3 °C and calculated from transducer data it was 36.18 °C and difference between measured and estimated it was 0.12 °C.

#### 4. Discussion

During the experiment, transducer thermistors' impedance was measured by a high-accuracy gauge Fluke type Black Stack used in laboratory environment. For practical measurements in the transducer design less precise, inexpensive ADC converters and a microprocessor can be used. Therefore, it is likely to achieve accuracy in range  $\pm(0.2)$  °C.

In the [19] study was shown, that the mean values and SD of the results of the measurement of the muscle temperature of the eight subjects after cooling with 5 minutes with ice pack were  $34.9 \pm 1.2$  °C. The temperature probe of thermometer (accuracy  $\pm 1$  °C) was inserted through the subcutaneous fat layer 1 cm into the muscle. In the studio [20], the muscle temperature was measured at a depth of 3 cm with a thermometer with accuracy  $\pm 0.1$  °C and a measurement value and SD submitted with one significant decimal place. The submitted averages of standard deviation were 0.7–1.2 °C.

Based on the results of the investigations, it can be stated that the temperature of the deeper layers of the muscle in most cases was measured in an invasive manner with an accuracy of  $\pm 0.1$  °C. The proposed transducer would allow the measured muscle temperature to be at a depth of 3 cm with similar accuracy. For measurement temperature of the muscles at different depths transducer it must be calibrated appropriately.

#### 5. Conclusions

The accuracy, similar to that of an invasive method using needle probes, can be achieved by measuring the temperature in deeper muscle layers using the proposed transducer.

**Author Contributions:** conceptualization and methodology Dumciene, A., conducting experiments, writing, review, editing Sipaviciene, S.

**Acknowledgments:** The authors would like to thank the colleagues from the Laboratory of measurement technology at Kaunas University of Technology for their assistance in conducting experiments.

**Conflicts of Interest:** The authors declare no conflict of interest.

## References

1. Teunissen, L.P.J.; Klewer, J.; de Haan, A.; de Koning, J.J.; Daanen, A.M. Non-invasive continuous core temperature measurement by zero heat flux. *Physiological measurement*. **2011**, *32*, 559–570. Available online: <http://dx.doi.org/10.1088/0967-3334/32/5/005>
2. Aadal, L.; Fog, L.; Pedersen, A.R. Tympanic ear thermometer assessment of body temperature among patients with cognitive disturbances. An acceptable and ethically desirable alternative? *Scand J Caring Sci*. **2016**, *30*, 766–773.
3. Erdling, A.; Johansson, A. Core Temperature—The Intraoperative Difference Between Esophageal Versus Nasopharyngeal Temperatures and the Impact of Prewarming, Age, and Weight: A Randomized Clinical Trial. *AANA Journal*. **2015**, *83*, 99–105.
4. Yeoh, W.K.; Lee, J.K.W.; Lim, H.Y.; Gan, C.W.; Liang, W.; Tan, K.K. Re-visiting the tympanic membrane vicinity as core body temperature measurement site. *PLoS ONE*. **2017**, *12*(4): e0174120. Available online: <https://doi.org/10.1371/journal.pone.0174120>
5. Flaifel, H.A.N.; Ayoub, F. Esophageal temperature monitoring. *M.E.J. ANESTH*. **2007**, *19*, 123–147.
6. Steck, L.N.; Sparrow, E.M.; Abraham, J.P. Non-invasive measurement of the human core temperature. *Int. J. Heat and Mass Transfer*, **2011**, *54*, 975–982. Available online: <http://dx.doi.org/10.1016/j.ijheatmasstransfer.2010.09.042>
7. Kitamura, K.I.; Zhu, I.; Chen, W.; Nemoto, T. Development of a new method for the noninvasive measurement of deep body temperature without a heater. *Medical Engineering & Physics*. **2010**, *32*, 1–6. Available online: <http://dx.doi.org/10.1016/j.medengphy.2009.09.004>
8. Guschlbauer, M.; Maul, A.C.; Yan, X.; Herff, H.; Annecke, T.; Sterner-Kock, A.; et al. (2016) Zero-Heat-Flux Thermometry for Non-Invasive Measurement of Core Body Temperature in Pigs. *PLoS ONE*. **2016**, *11*(3):e0150759. doi:10.1371/journal.pone.0150759
9. Nakamura, S.; Nakamura, M.; Maeda, E.; Nikawa, Y. Study on Temperature Measurement Using MRI during Acupuncture and Moxibustion. *Electronics and Communications in Japan*. **2017**, *100*, 62–67.
10. Komiya, H.; Maeda, J.; Suzuki, I. Development of multi-frequency impedance method of measuring muscle temperature noninvasively. *Advances in Exercise & Sports Physiology Date*. **2014**, *15*, 1–2. Available online: <http://web.b.ebscohost.com/ehost/pdfviewer/pdfviewer?vid=4&sid=fd567c98-7d63-42eb-95e3-2d5c1b931d02%40sessionmgr101>
11. Buono, M.J.; Jechort, A.; Marques, R.; Smith, C.; Welch J. Comparison of infrared versus contact thermometry for measuring skin temperature during exercise in the heat. *Physiol Meas*. **2007**, *28*, 855–859. Available online: <https://doi.org/10.1088/0967-3334/28/8/008>
12. Bach, A.J.E.; Stewart, I.B.; Disher, A.E.; Costello, J.T. A comparison between conductive and infrared devices for measuring mean skin temperature at rest, during exercise in the heat, and recovery. *PLoS One*. **2015**, *10*: e0117907. Available online: <https://doi.org/10.1371/journal.pone.0117907>
13. Tomchuk, D.; Rubley, M.D.; Holcomb, W.R.; Guadagnoli, M.; Tarno, J.M. The magnitude of tissue cooling during cryotherapy with varied types of compression. *Journal of Athletic Training*, **2010**, *45*, 230–237. Available online: <http://dx.doi.org/10.4085/1062-6050-45.3.230>
14. Ramanauskiene, I.; Skurvydas, A.; Sipaviciene, S.; Senikiene, Z.; Linonis, V.; Krutulyte, G.; Vizbaraite, D. Influence of heating and cooling on muscle fatigue and recovery. *Medicina (Kaunas)*. **2008**, *44*, 687 – 693.
15. Dumciene, A.; Sipaviciene, S. Deeper-Layer Body Tissue Temperature Control Using Multi-Sensory Transducer. *Elektronika ir Elektrotechnika*. **2015**, *21*, 24–27.

16. Pennes, H.H. Analysis of Tissue and Arterial Blood Temperature in the Resting Human Forearm. *J. of Applied Physiology*, **1948**, 1, 93–102.
17. McIntosh, R.L.; Anderson, V. A comprehensive tissue properties database provided for the thermal assessment of a human at rest. *Biophysical Reviews and Letters*. **2001**, 5, 129–151.
18. Lakhssassi, A.; Kengne, E.; Semmaoui, H. Modified pennes' equation modelling bio-heat transfer in living tissues: analytical and numerical analysis. *Natural Science*. **2010**, 2, 1375-1385.
19. Mars, M.; Hadebe, B.; Tufts, M. The effect of icepack cooling on skin and muscle temperature at rest and after exercise. *SAJSM*, **18**, **2006**, 60–66.
20. Costello, J.T.; Culligan, K.; Selfe, J.; Donnelly, A.E. (2012) Muscle, Skin and Core Temperature after 210 °C Cold Air and 8 °C Water Treatment. *PLoS ONE*, **2012**, 7(11): e48190. doi:10.1371/journal.pone.0048190